ACCOUNTS
—of materials research—

pubs.acs.org/amrcda

Article

Nanoparticle Transport in Polymer Solutions

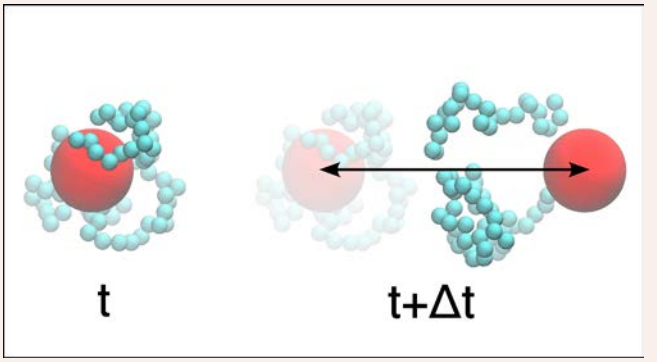
Jacinta C. Conrad,* Ryan Poling-Skutvik,* Mohammadjavad Haji Rezaei, Shivraj B. Kotkar, and Jeremy C. Palmer*

Cite This: https://doi.org/10.1021/accountsmr.6c00189

Read Online

ACCESS | Metrics & More | Article Recommendations

CONSPECTUS: Polymer solutions are essential materials both for their uses in industries ranging from energy storage to consumer products to additive manufacturing and as model physical systems that can mimic biological tissues and hydrogels with well-controlled structures, dynamics, and properties. Nanoparticles are commonly added to these solutions to impart functionality, deliver theranostics, or manipulate mechanical properties, all of which require a fundamental understanding of nanoparticle transport through the surrounding polymer mesh. Over recent decades, nanoparticle dynamics have been analyzed using the framework of microrheology to measure the local viscoelasticity of complex fluids. In contrast to homogeneous, Newtonian fluids in which particle dynamics are described through the Stokes−Einstein-Sutherland (SES) relationship, the structural heterogeneity and viscoelasticity of polymer solutions lead to significant deviations with nanoparticles transporting up to 1,000× faster than expected from the bulk solution viscosity. These deviations dramatically alter how nanoparticles disperse and distribute through complex environments and introduce significant discrepancies between microrheological measurements and bulk mechanical properties. The vast combinatorial library of polymer chemistries, architectures, and solution formulations necessitates predictive understanding of nanoparticle transport and how it relates to the underlying physicochemical interactions.



In this Account, we describe theoretical advances and summarize experimental and simulation findings that build a comprehensive understanding of nanoparticle transport in polymer solutions. The key insight is that nanoparticle transport can be better understood by considering the *local* dynamics and structure of the polymer solution rather than the bulk viscoelasticity. Specifically, we show that nanoparticles violate the SES relationship because they are comparable in size to structural heterogeneities and instead exhibit a size-dependent diffusivity. Using theoretical predictions derived from polymer scaling theory, the faster dynamics are related to the ratio between nanoparticle size and the polymer correlation length ξ because the nanoparticles couple to segmental fluctuations of the polymer mesh. Despite the success of this coupling theory in describing the long-time diffusivity of nanoparticles, it does not capture the dynamics on short time scales, on which nanoparticles move subdiffusively. On these time scales, the nanoparticles not only couple to segmental fluctuations but also to the center-of-mass dynamics of the polymer coils. To expand these findings across the formulation library, we detail some impacts of nanoparticle surface interactions and polymer conformation and chemistry on this modified coupling theory. The stiffness and charge of the surrounding polymer and the softness of the particle all affect how nanoparticle dynamics couple to those of the polymers. Looking forward, we identify open questions that motivate theoretical considerations and directions for experimental and simulation thrusts toward the ultimate goal of fully describing, predicting, and tailoring nanoparticle transport in polymer solutions and other heterogeneous complex fluids for applications in medicine, energy, and advanced materials.

INTRODUCTION

Diffusion of nanoscale particles in macromolecule-laden environments determines the efficacy of theranostic delivery through mucus[1] and tumors[2,3] as well as the ability to manufacture battery cathodes[4] and functional nanocomposites[5−7] (Figure 1). Fundamental understanding of the factors that dictate diffusive transport of nanoparticles in medicine, energy, and materials remains limited, however, by the variations in macromolecule size, chemistry, dispersity, and concentration along with particle size, shape, and surface chemistry.

Received: July 9, 2026
Revised: September 21, 2026
Accepted: October 8, 2026

ACS Publications

© XXXX Accounts of Materials Research. Co-published by ShanghaiTech University and American Chemical Society. All rights reserved.

Downloaded from pubs.acs.org/amrcda/article-pdf/doi/10.1021/accountsmr.6c00189/6900460/accountsmr.6c00189.pdf by UNIV OF RHODE ISLAND user on 29 October 2026

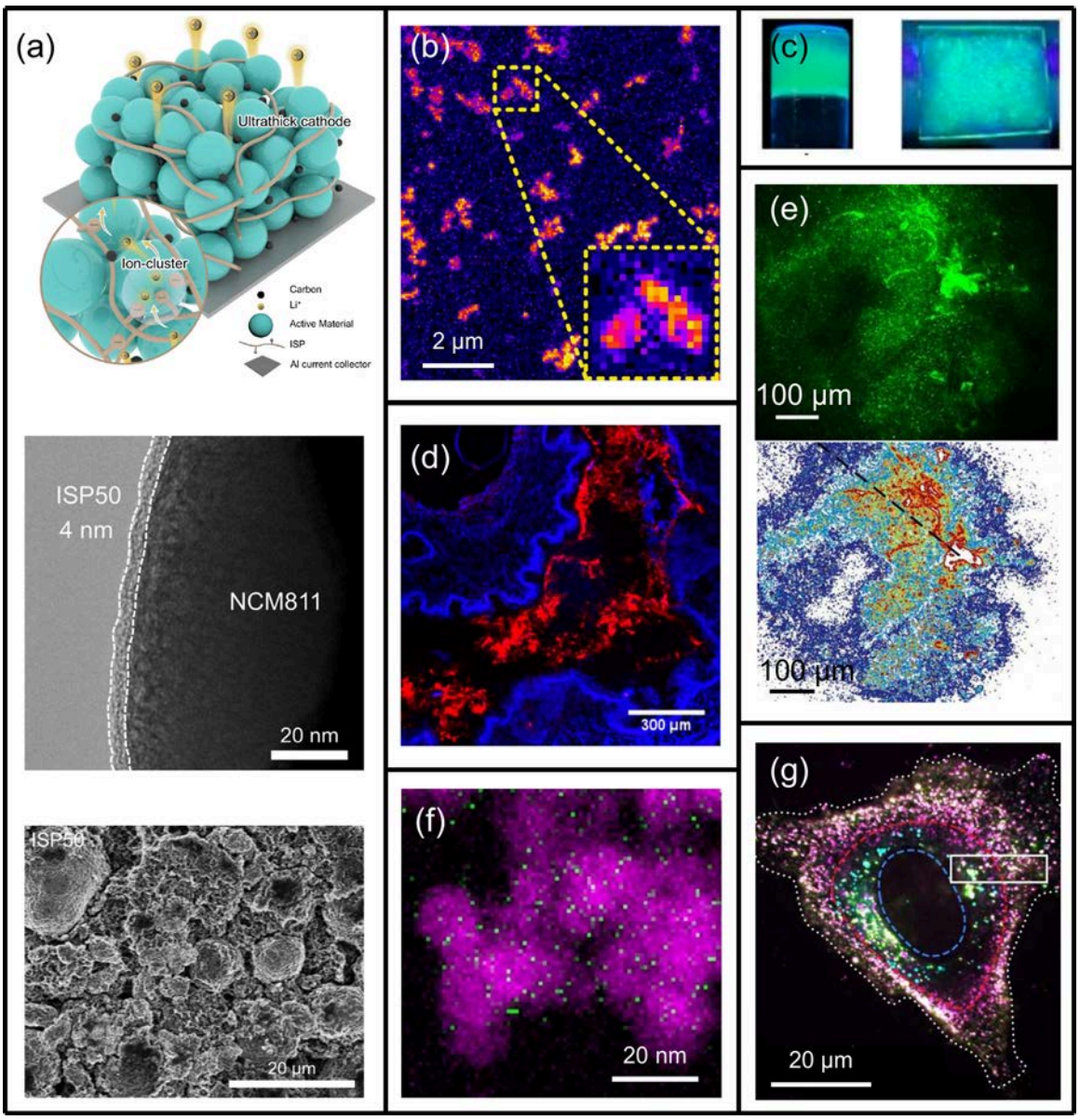


Figure 1. Practical applications of nanoparticle transport in medicine, energy, and materials. (a) (Top) Schematic diagram of ion clusters in an ionic copolymer/NCM811 metal oxide cathode, (middle) TEM image of the copolymer/NCM811 interface, and (bottom) SEM image of the copolymer/NCM811 cathode. Reproduced with permission from ref 4. Copyright 2025 Royal Society of Chemistry. (b) Maximum projected fluorescence intensity of rhodamine 6G tracer molecules in polyvinylpyrrolidone thin films; inset shows an enlarged area of 1 μm^2. Reproduced from ref 5. Copyright 2013 American Chemical Society. (c) Fluorescein/ZIF-8/laponite hydrogel nanocomposite. Reproduced from ref 6. Copyright 2018 American Chemical Society. (d) Distribution of poly(ethylene glycol)-functionalized polystyrene nanoparticles in the vaginal mucus of mice in diestrus. Reproduced from ref 2. Copyright 2013 American Chemical Society. (e) Fluorescence (top) and heat map (bottom) images of quantum dot gelatin nanoparticles injected into an HT-1080 tumor. Reproduced from ref 1. Copyright 2010 Wong, Stylianopoulos, Cui, Martin, Chauhan, Jiang, Popović, Jain, Bawendi, and Fukumura. (f) Chemical bonding map of silica-filled styrene−butadiene rubber. Reproduced from ref 7. Available under a CC-BY 4.0 license [https://creativecommons.org/licenses/by/4.0/]. Copyright 2020 Sato, Kuwauchi, Miyoshi, and Jinnai. (g) Lipid nanoparticles injected into HeLa cells; white outline indicates the cell border, red outline indicates the perinuclear region, and blue outline indicates the nucleus. Reproduced from ref 3. Available under a CC-BY 4.0 license [https://creativecommons.org/licenses/by/4.0/]. Copyright 2025 Johansson, Du Rietz, Hedlund, Eriksson, Oude Blenke, Pote, Harun, Nordenfelt, Lindfors, and Wittrup.

Our work has focused on elucidating the mechanisms controlling nanoparticle diffusion in well-characterized solutions of model polymers. Polymer solutions are a particularly convenient model for macromolecule-laden environments because the length scales and dynamics (shown schematically in Figure 2) can be measured via scattering and rheology and predicted using polymer scaling theories.[8] Structurally, in dilute solutions the polymers are characterized by the radius of gyration R_g, which scales with the number of repeat units N as $R_g \sim N^{\nu}$; here the Flory exponent ν (which is the inverse of the fractal dimension $d_f = 1/\nu$) is 1/3 for a globule, 1/2 for a random coil (i.e., a polymer in a θ-solvent or melt), 0.588 for a self-avoiding random walk (i.e., a polymer in a good solvent), and 1 for a rigid rod. When the coils begin to overlap at the overlap concentration c^*, a second length scale emerges: the correlation length ξ characterizing the average distance between monomers

https://doi.org/10.1021/accountsmr.6c00189
Acc. Mater. Res. XXXX, XXX, XXX−XXX

Downloaded from pubs.acs.org/amrcda/article-pdf/doi/10.1021/accountsmr.6c00189/6900460/accountsmr.6c00189.pdf by UNIV OF RHODE ISLAND user on 29 October 2026

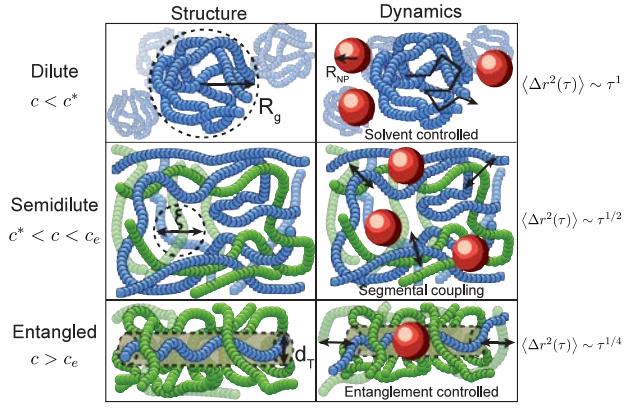


Figure 2. Schematic of the dilute, semidilute, and entangled concentration regimes for polymer solutions.

on neighboring polymer chains. For polymer concentrations exceeding the entanglement concentration c_e, the solution is described by a third length scale, the tube diameter d_T,[9] which describes the strength of confinement imposed by neighboring, highly interpenetrated polymers and is typically 5−10ξ. The ratios R_{NP}/R_g, R_{NP}/ξ, and R_{NP}/d_T are the natural candidates for dimensionless length scales in the dilute, semidilute, and entangled regimes, respectively.

Dynamically, the local mean-square displacement (MSD) $\Delta r^2(\tau) \equiv \langle (\mathbf{r}(\tau + t) - \mathbf{r}(t))^2 \rangle$ of the monomers depends on concentration. The simplest models for polymer dynamics treat the polymer as a series of beads connected by springs: in the Rouse model, the beads experience only frictional interactions with other beads, whereas in the Zimm model the beads additionally feel hydrodynamic interactions (HI). On length scales below ξ, the monomers experience HI due to the solvent but screened by other monomers; the MSD of the monomers on these intermediate time scales exhibits a power-law dependence on time, $\Delta r^2(\tau) \sim \tau^{2/3}$, as described by the Zimm model. HI are screened at distances exceeding ξ and thus the MSD at intermediate times follows $\Delta r^2(\tau) \sim \tau^{1/2}$, as described by the Rouse model. Finally, in entangled solutions where $c > c_e$, polymers move along their contour to relax by reptation within the tube formed by their neighbors, and the monomer MSD follows $\Delta r^2(\tau) \sim \tau^{1/4}$ (combining Rouse and reptation models) and then $\sim \tau^{1/2}$ (reptation alone) before a terminal diffusive regime.[10] Thus, both solution structure and dynamics can be tuned through the degree of polymerization N, the scaling exponent ν (a measure of solvent quality), and polymer concentration c.

NANOPARTICLES DIFFUSE FASTER THAN PREDICTED

The MSD of a particle of radius R_{NP} in a homogeneous liquid with viscosity η is $\langle \Delta r^2(\tau) \rangle = 2dD\tau$ for d dimensions. The diffusivity D is given by the Stokes−Einstein−Sutherland (SES) relationship $D = k_B T/6\pi\eta R_{NP}$, where k_B is Boltzmann's constant and T is the temperature. In a complex fluid (e.g., a polymer solution or network), the motion of sufficiently large particles follows the generalized Stokes−Einstein relationship (GSER)[11] $\langle \Delta \tilde{r}^2(s) \rangle = 3k_B T/3\pi s^2 \tilde{\eta}(s)$, where the tilde symbols indicate the Laplace transform.[12] To satisfy the assumptions underlying the Stokes component of the GSER, which describes the effects of HI, the probe particle must be larger than any of the characteristic length scales in the fluid. In practice, this assumption is satisfied when R_{NP} is 3−5 times the polymer length scale.[13,14] Thus, micron-sized particles typically follow GSER, but nanoparticles with sizes comparable to polymeric length scales such as R_g, ξ, and d_T often violate this assumption so that the dynamics can no longer be described by GSER.

Many researchers have measured the diffusion of spherical nanoparticles in aqueous and nonaqueous solutions of polymers and polymer melts of various chemistries and molecular weights.[15−24] These and similar experiments reveal at least three ways in which nanoparticle diffusion deviates from SES/GSER behavior. First, when polymers are attracted to the nanoparticles, they form a bound layer[25] that increases the size of the diffusing nanoparticle and slows diffusion.[26] The size of the bound layer, inferred from the change in diffusivity, is comparable to the polymer R_g.[26] More puzzling are two other observations. Second, nanoparticles often diffuse markedly faster than predicted from the bulk viscosity of a polymer solution or melt using SES/GSER (Figure 3(a)).[17] Last, this deviation from bulk viscosity can sometimes exhibit a maximum with increasing polymer concentration[27] before approaching the SES prediction at sufficiently high polymer concentration (Figure 3(b)). Thus, diffusion even of spherical nanoparticles in polymer matrices can exhibit surprising, noncontinuum features that depend on both particle size and the properties of the medium, including polymer chemistry, molecular weight, and the presence or absence of solvent (i.e., a solution or melt).

THEORETICAL PICTURES FOR NANOPARTICLE DIFFUSION

The surprising deviations from SES were first described using phenomenological models that attributed diffusive slowing to geometry or to hydrodynamic interactions. For example, obstruction models posit that particles adopt tortuous trajectories that slow diffusion to move around rigid polymer coils.[28,29] Hydrodynamic models,[16,30,31] by contrast, posit that highly dynamic polymers interact with particles by increasing the viscous drag at the particle surface. As a result, particle diffusion decreases with polymer concentration according to $D/D_0 = \exp[(L/\xi)^b]$ where L is a characteristic length scale that depends on particle and polymer properties,[19,20] b is an empirical fitting parameter, and ξ is the length scale over which HI are screened. Both obstruction and hydrodynamic models capture changes in particle dynamics in polymer solutions but require empirical measurements and lack predictive capabilities over broad concentration ranges and polymer chemistries. These models can be modified to account for depletion layers that enable particles to move rapidly through the solvent layer on short time scales.[32] On longer time and length scales, however, particles and their depletion layers are slowed down by the surrounding polymer mesh. Thus, the long-time dynamics must depend on a characteristic length scale.

An alternative approach is to model the dynamics of the polymers along with those of the particles. Scaling models[8,33,34] extend hydrodynamic theories to include single-chain polymer relaxations around the particle. The coupling theory of Cai, Panyukov, and Rubinstein (CPR)[33] proposed that the dynamics of particles whose size lies between ξ and d_T depends on relative time scales. For very short times, particles diffuse in the solvent until encountering the polymer mesh. The particles begin to interact with polymer segments of size ξ on the time scale at which correlation blobs relax, $\tau_\xi = \eta_0 \xi^3/k_B T$. For $t > \tau_\xi$, particles

Downloaded from pubs.acs.org/amrcda/article-pdf/doi/10.1021/accountsmr.6c00189/6900609/accountsmr.6c00189.pdf by UNIV OF RHODE ISLAND user on 29 October 2026

https://doi.org/10.1021/accountsmr.6c00189
Acc. Mater. Res. XXXX, XXX, XXX−XXX

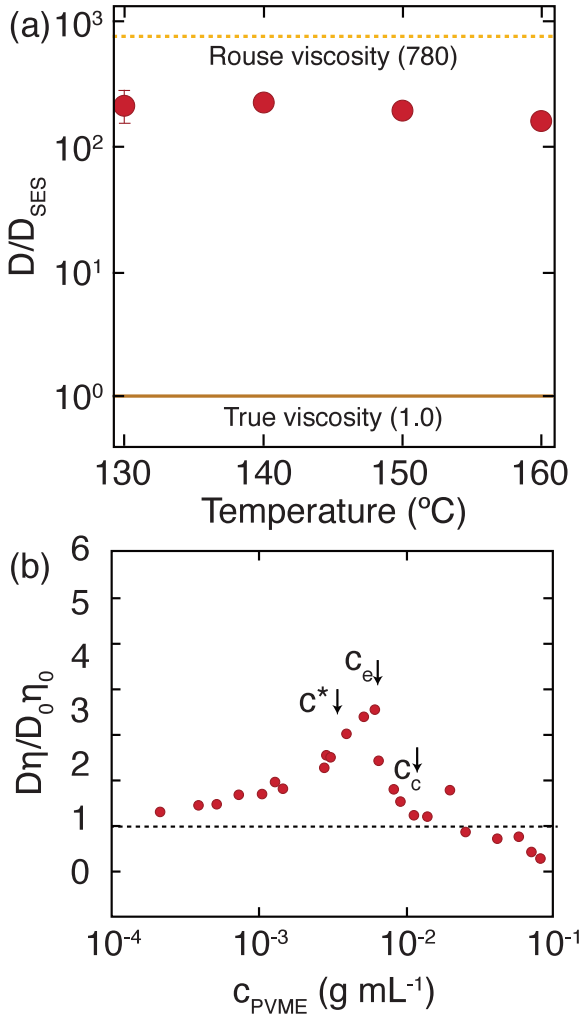


Figure 3. The diffusivity of spherical nanoparticles shows surprising deviations from predictions of continuum hydrodynamics. (a) Normalized diffusivity D/D_{SES} as a function of temperature for cadmium selenide quantum dots in a polystyrene melt. Horizontal lines indicate the values of viscosity used to calculate the SES diffusivity D_{SES}: the pure polymer viscosity (true viscosity) or the pure polymer viscosity without entanglements (Rouse viscosity). Adapted from ref 17. Copyright 2007 American Chemical Society. (b) Product of nanoparticle diffusivity D and solution viscosity η normalized by the corresponding values at infinite dilution for polystyrene spheres in solutions of poly(vinyl methyl ether) as a function of polymer concentration c_{PVME}. Dashed line indicates the SES relation. $c_c \approx 2c_e$ is the concentration at which SES behavior is recovered. Adapted from ref 27. Copyright 1994 American Chemical Society.

are localized by segments of the polymer chain that relax on a time scale $t \approx \tau_\xi(N/N_\xi)^2$, where N is the number of monomers in the chain and N_ξ is the number of monomers in a correlation blob. Larger sections of the polymer chain relax and hence interact with particles on longer time scales, such that the effective viscosity felt by particles increases with time as $\eta_{eff}(t) \sim \eta_0(t/\tau_\xi)^{1/2}$. Particle and polymer dynamics decouple once the polymer relaxes over the polymer size on a time scale $\tau_R \approx \tau_\xi(2R_{NP}/\xi)^4$. Thereafter the particle dynamics depend on the effective viscosity $\eta_{eff} \approx \eta_0(2R_{NP}/\xi)^2$.

Finally, variations on mode-coupling theory (MCT) relate nanoparticle dynamics to collective density fluctuations in the polymer solution that are obtained from the polymer structure. Using a simplified version of MCT,[35] the long-time diffusion coefficient of nanoparticles in solutions of flexible polymers was calculated as $D = D_{micro} + D_{hydro}$, where D_{micro} includes effects arising from binary collisions and solvent density and D_{hydro} includes contributions from the solvent transverse current.[36] In a different approach, self-consistent Langevin equations were used to relate the resistance of particles moving through a polymer melt to the microstructure melt structure and the length-scale-dependent relaxation time of collective density fluctuations.[14,37] These approaches reproduce long-time diffusion coefficients, although their ability to capture short-time dynamics is limited because the calculations depend sensitively on the dynamic propagator of collective density fluctuations.[14]

TESTS USING EXPERIMENTS AND SIMULATIONS

We tested the applicability of these theoretical pictures in experiments by measuring the dynamics of nanoparticles of various sizes as they diffused in aqueous solutions of partially hydrolyzed polyacrylamide (HPAM, M_w = 8 MDa) using optical microscopy.[38,39] HPAM's radius of gyration at infinite dilution $R_{g,0}$ = 270 nm is comparable in size to particles that can be optically resolved in fluorescence microscopy images and tracked over time. Thus, by using particles of diameter $2R_{NP}$ = 300 nm to 2 μm, we were able to access a range of particle-to-polymer size ratios. From the particle trajectories, we calculated the MSDs. On long time scales, $\langle \Delta x^2(\Delta t)\rangle \propto \Delta t$ and we determined the diffusivity D from the slope. We found that D/D_{SES} increasingly deviates from the SES prediction as polymer concentration is increased or size is decreased (Figure 4(a)). This result confirms earlier observations of faster-than-SES behavior[17,20,40] and establishes the systematic deviation from SES that arises in polymer solutions.

To understand the origin of the non-SES dynamics, we examined our data as a function of the theoretical predictions[33] and data collapses[16,18−20] used by a variety of research groups to understand the physics controlling nanoparticle diffusion. We found that our data collapsed cleanly as a function of the scaling variable $2R_{NP}/\xi$. Specifically, $D/D_0 \sim (2R_{NP}/\xi)^{-2}$, as predicted by CPR coupling theory,[33] for all but the largest 2 μm particles (which do not satisfy the size criterion required for this scaling behavior and instead follow SES). This collapse thus suggested that the long-time dynamics of the nanoparticles are controlled by the relaxations of polymer segments over the nanoparticle length scale.

Although the long-time diffusive dynamics could be well predicted, the short time particle dynamics proved more complicated. On short time scales, the particle dynamics are subdiffusive, i.e. $\langle \Delta x^2(\Delta t)\rangle \propto \Delta t^\alpha$ with $\alpha < 1$. CPR coupling theory predicted this subdiffusion arises due to coupling with Rouse modes so that $\alpha = 1/2$, as previously observed for particles bound directly to a polymer network.[41] The largest 2 μm particles indeed exhibit short time subdiffusive exponents near $\alpha = 1/2$ at sufficiently high polymer concentration (Figure 5(a)). Smaller particles, however, have $\alpha > 1/2$ for all polymer concentrations, and α decreases with increasing polymer concentration or increasing particle size. To confirm that the deviation from $\alpha = 1/2$, we also conducted X-ray photon correlation spectroscopy experiments on smaller particles (silica nanoparticles of diameter 48 nm in unentangled solutions of polystyrene in 2-butanone) and observed $\alpha \approx 0.63$,[42] again

Downloaded from pubs.acs.org/amrcda/article-pdf/doi/10.1021/accountsmr.6c00189/6900609/accountsmr.6c00189.pdf by UNIV OF RHODE ISLAND user on 29 October 2026

https://doi.org/10.1021/accountsmr.6c00189
Acc. Mater. Res. XXXX, XXX, XXX−XXX

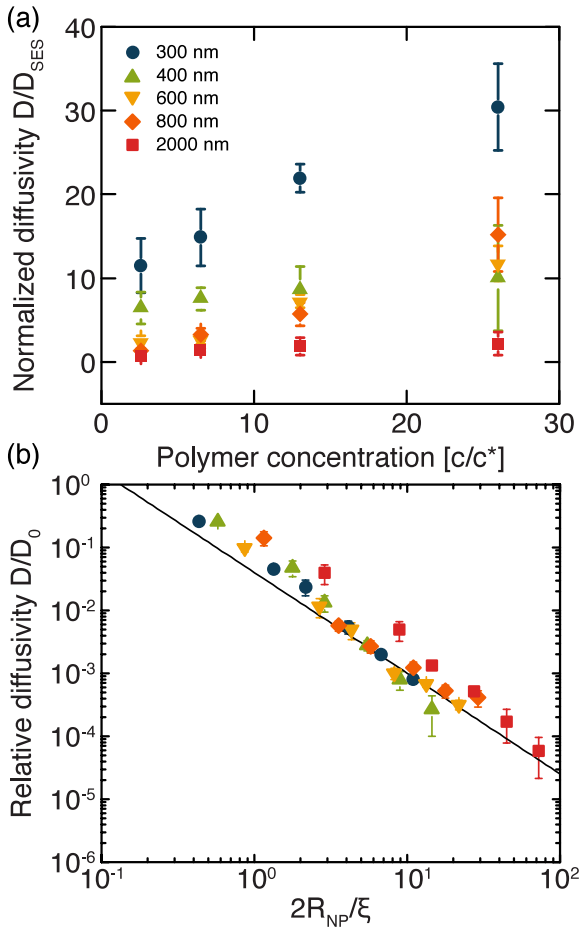


Figure 4. Nanoparticles diffuse faster than expected in polymer solutions. (a) Diffusivity of nanoparticles normalized by the SES diffusivity D/D_{SES} as a function of polymer concentration c/c^* for PS particles of various diameters, as indicated in the legend, diffusing in aqueous HPAM (M_w = 8 MDa) solutions. (b) Diffusivity of nanoparticles normalized by the diffusivity in pure solvent D/D_0 as a function of the ratio of the nanoparticle diameter to the polymer correlation length $2R_{NP}/\xi$. The solid line indicates the slope of −2 predicted by ref 33. Reproduced from ref 39. Copyright 2015 American Chemical Society.

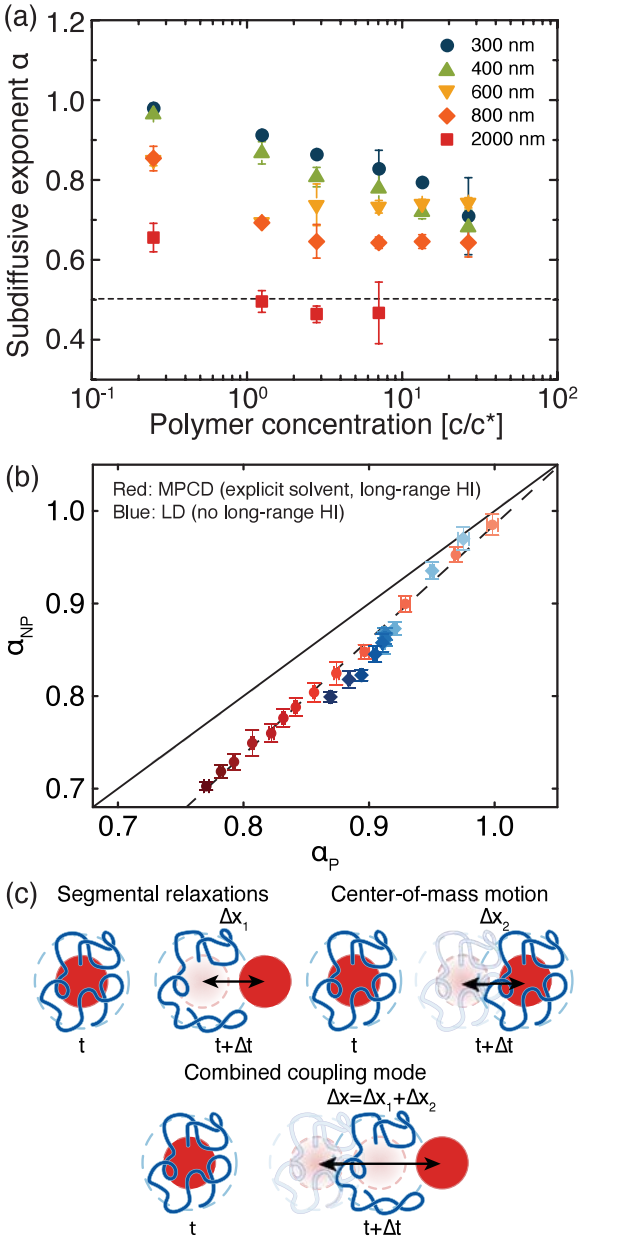


Figure 5. Nanoparticle dynamics couple to polymer center-of-mass dynamics on short time scales. (a) Subdiffusive exponent α as a function of normalized polymer concentration c/c^* for PS nanoparticles of various diameters diffusing in aqueous HPAM solutions (M_w = 8 MDa). Dashed line indicates $\alpha = 1/2$ predicted for particles coupled to Rouse relaxations. Reproduced from ref 39. Copyright 2015 American Chemical Society. (b) Subdiffusive exponent for the nanoparticles α_{NP} as a function of the subdiffusive exponent of the polymer centers-of-mass α_P obtained from MPCD simulations (red) and LD simulations (blue). (c) Nanoparticles couple to the center-of-mass relaxations of polymers of similar size in addition to the segmental dynamics. (b) and (c) are reproduced from ref 44. Copyright 2018 American Chemical Society.

larger than the CPR coupling prediction.[33] Subdiffusive particle dynamics have also been observed in highly entangled polymer solutions but with α deviating in the opposite direction; for $d_T \ll R_{NP}$, $\alpha < 0.5$ because particle dynamics are no longer coupled to Rouse relaxations but rather to the reptation of the entangled polymers.[43] These findings suggested that particle dynamics on short time scales cannot be fully explained by coupling to segmental fluctuations of the polymer mesh.

To address this unexpected complexity, we needed to characterize the polymer dynamics on time scales comparable to particle dynamics. Our experimental methods did not provide ready access to the relevant polymer dynamics. The polymers were unlabeled in our particle tracking measurements, and segmental dynamics are not accessible with conventional fluorescence microscopy. Likewise, although our SiO_2/PS/2-butanone system[45] was designed to enable neutron scattering measurements of polymer structure and dynamics, contrast-matched neutron spin−echo (NSE) spectroscopy was unable to resolve dynamics on sufficiently long length scales comparable to that of optical microscopy or XPCS. At the time, NSE had a maximum temporal resolution of ∼100 ns whereas optical microscopy and XPCS were limited by camera frame rates to ≳1 ms. Although beamline upgrades and instrument improvements have significantly improved the temporal resolution of these methods over the past decade, at the time, this gap of 4 orders of magnitude in temporal resolution precluded complementary characterizations of both nanoparticle and polymer dynamics

https://doi.org/10.1021/accountsmr.6c00189
Acc. Mater. Res. XXXX, XXX, XXX−XXX

Downloaded from pubs.acs.org/amrcda/article-pdf/doi/10.1021/accountsmr.6c00189/6900460/accountsmr.6c00189.pdf by UNIV OF RHODE ISLAND user on 29 October 2026

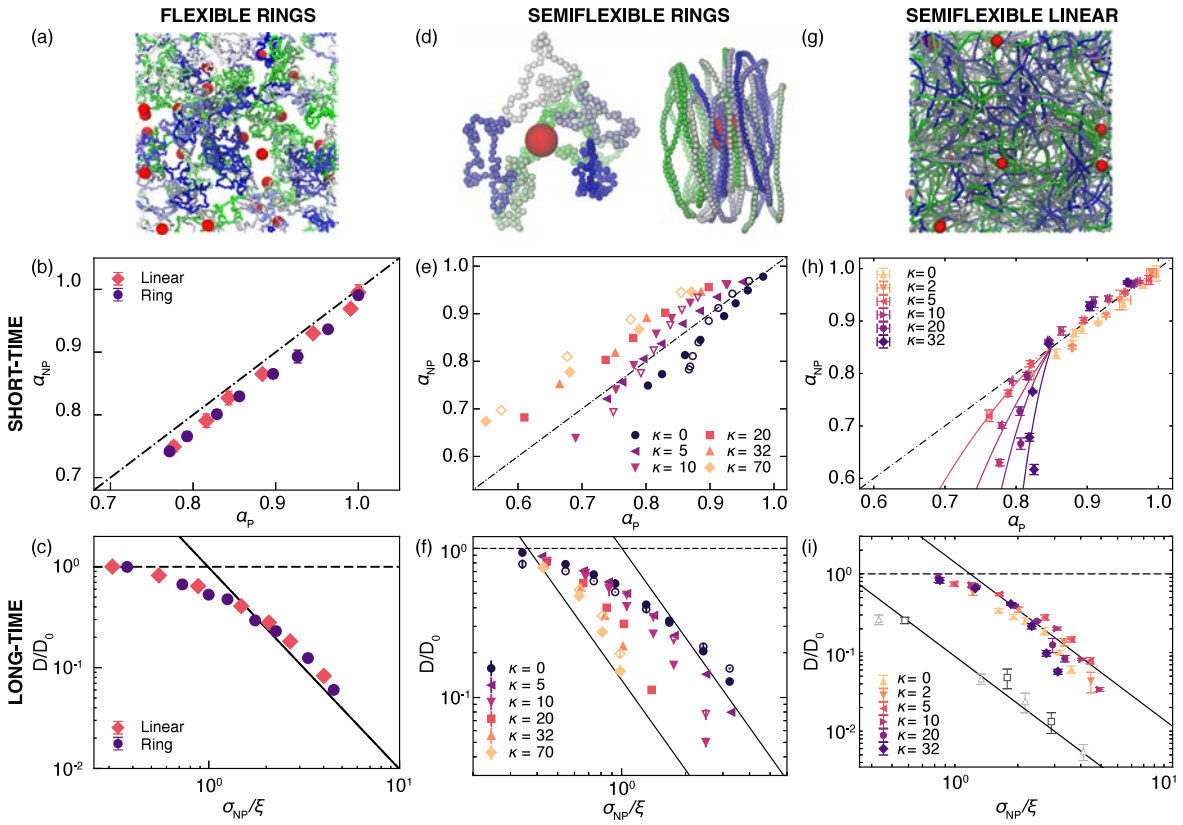


Figure 6. Testing the coupling picture using hybrid MD-MPCD simulations for (a–c) flexible ring, (d–f) semiflexible ring, and (g–i) semiflexible linear polymers. (a, d, g) Illustration of nanoparticles in solutions of (a) flexible ring polymers, (d) ring polymers with stiffness parameter κ = (left) 0 and (right) 70, and (g) semiflexible linear polymers with $\kappa = 32$. (b, e, h) Subdiffusive exponent of the nanoparticles α_{NP} versus subdiffusive exponent α_P of the polymer center-of-mass. Dashed lines indicate the line $\alpha_{NP} = \alpha_P$. (c, f, i) Normalized diffusivity D/D_0 versus particle diameter normalized by polymer correlation length σ_{NP}/ξ; solid lines indicate the $D/D_0 \sim (\sigma_{NP}/\xi)^{-2}$ scaling of ref 33. The comparison in (c) is made at equal monomer concentration. Open symbols in (e, f) are LD simulations (without many-body HI). Open symbols in (i) are the experimental data from ref 39. (a–c) are reproduced with permission from ref 48. Copyright 2021 AIP. (d–f) are reproduced from ref 50. Copyright 2024 American Chemical Society. (g–i) are reproduced with permission from ref 51. Copyright 2019 Chen, Poling-Skutvik, Howard, Nikoubashman, Egorov, Conrad, and Palmer.

necessary to experimentally test the dynamic coupling in the subdiffusive regime.

Instead, we used computer simulation, which can provide the necessary spatiotemporal resolution, to investigate coupling between nanoparticle and polymer dynamics in solution. We employed multiparticle collision dynamics (MPCD), which is a mesoscale simulation method that uses a highly simplified solvent model to produce HI at reduced computational cost.[46] Instead of interacting by conventional pairwise forces, the solvent particles periodically undergo collective momentum-exchanging collisions within spatially localized cells according to a prescribed rule. Many collision rules have been proposed,[46] including the well-known stochastic rotation dynamics (SRD) approach.[47] The collision rules all conserve mass and linear momentum, allowing many-body hydrodynamic correlations to develop.[46] Solutions of nanoparticles and polymers are simulated in MPCD with a hybrid scheme that uses standard molecular dynamics (MD) to propagate their motions with coupling to the MPCD solvent.[44,46] Through this hybrid MD-MPCD approach, we simulated the dynamics of both nanoparticles and polymers over the same spatiotemporal scales. We found that the centers-of-mass for polymer chains in semidilute solutions exhibit subdiffusive dynamics on short time scales and diffusive dynamics on long time scales, reminiscent of the behavior of the nanoparticles.

The key physical insight from the simulations is that the subdiffusive exponent of the nanoparticles α_{NP} is linearly proportional to that of the polymer center-of-mass α_P (Figure 5(b)).[44] This coupling holds both for MPCD simulations that include many-body HI as well as for complementary Langevin dynamics (LD) simulations that account for the viscous drag and restoring Brownian forces resulting from interactions with the solvent but not many-body HI. This result shows that the nanoparticles couple to the polymer center-of-mass dynamics on short time and length scales as well as to segmental relaxations (Figure 5(c)). For polymers, segmental relaxations are the predominant dynamic mode on short time scales, whereas center-of-mass diffusion only becomes important on longer time scales. Nanoparticles, however, can couple to both dynamic modes because the segmental relaxations must occur over the nanoparticle length scale. The corresponding time scale τ_R is comparable to the diffusive time scale for the polymer center-of-mass. This observation that nanoparticles couple to multiple dynamic modes of the polymer resolves the unexpectedly large subdiffusive exponents for nanoparticle transport on short time scales. Additionally, although HI indeed modify the relaxation spectrum of the surrounding polymers, they do not affect the coupling between the subdiffusive dynamics of the polymer center-of-mass and those of the nanoparticle (Figure 5(b)). Because the coupling is independent of HI, the same physical

https://doi.org/10.1021/accountsmr.6c00189
Acc. Mater. Res. XXXX, XXX, XXX−XXX

Downloaded from pubs.acs.org/amrcda/article-pdf/doi/10.1021/accountsmr.6c00189/6900460/accountsmr.6c00189.pdf by UNIV OF RHODE ISLAND user on 29 October 2026

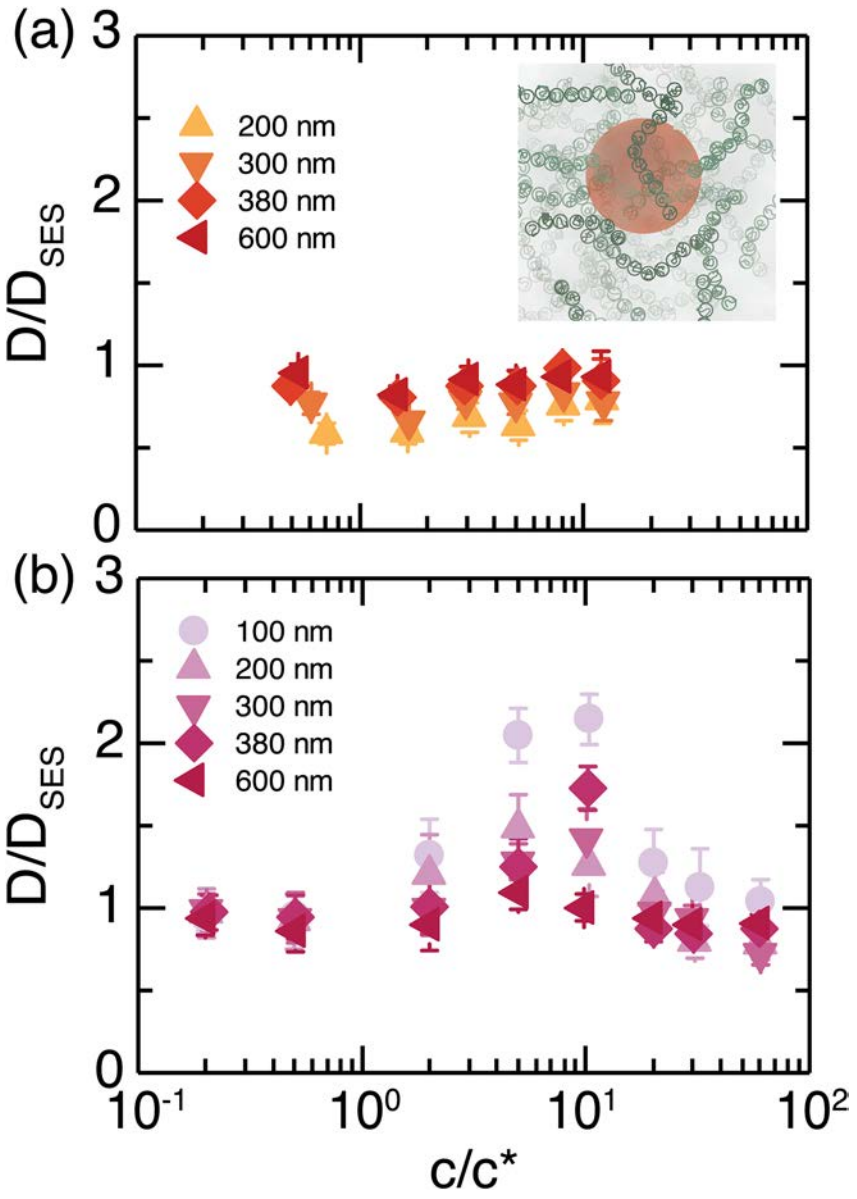


Figure 7. Normalized diffusivity D/D_{SES} as a function of normalized polymer concentration c/c^* for polystyrene particles diffusing in solutions of sodium poly(styrenesulfonate) of M_w = 2.2 MDa in (a) a solution with ionic strength 10^{-1} M and (b) with no added salt. Inset: schematic of a nanoparticle in a polyelectrolyte solution, showing the extended conformation. Reproduced from ref 52. Copyright 2020 American Chemical Society.

picture can unify the dynamics observed in semidilute solutions and those in polymer melts, where HI are fully screened.

LIMITS OF APPLICABILITY OF THE COUPLING PICTURE

CPR coupling theory was developed to describe the simple scenario captured in our experiments: particles in solutions of nonadsorbing linear polymers of similar size. To test the broader applicability of this theory to other scenarios, we used our simulation approach to examine polymers of different properties beyond flexible and linear.

Some polymer properties do not affect the coupling of nanoparticle and polymer dynamics — for example, the lack of free chain ends. In solutions of flexible ring polymers (Figure 6(a)), the subdiffusive exponents of the nanoparticle and of the polymer center-of-mass dynamics are linearly proportional (Figure 6(b)), confirming their coupling on short time scales.[48] Likewise, the normalized diffusion coefficients D/D_0 of nanoparticles diffusing in solutions of linear versus ring polymers collapse onto a scaling curve as a function of the scaling variable σ_{NP}/ξ, where $\sigma_{NP} = 2R_{NP}$ is the nanoparticle diameter (Figure 6(c)), given two constraints. First, we compared linear and ring polymers with equal $R_{g,0}$ and total monomer concentration, required to ensure that the dynamics of nanoparticles were measured at equal crowding and that the polymer size was constant. Second, we computed the correlation length ξ for a solution of rings from the geometric pore size distribution.[49] Within these constraints, we concluded that the presence or absence of free chain ends does not strongly affect nanoparticle transport, even in the presence of concatenated rings. Instead, the segmental dynamics in both linear and ring polymers control nanoparticle transport.

By contrast, reducing the polymer flexibility markedly alters nanoparticle–polymer coupling. Intriguingly, these changes manifest differently in solutions of ring versus linear polymers. For ring polymers, α_{NP} and α_P remain linearly proportional as

Downloaded from pubs.acs.org/amrcda/article-pdf/doi/10.1021/accountsmr.6c00189/6900460/accountsmr.6c00189.pdf by UNIV OF RHODE ISLAND user on 29 October 2026

https://doi.org/10.1021/accountsmr.6c00189
Acc. Mater. Res. XXXX, XXX, XXX−XXX

the stiffness parameter κ is increased (Figure 6(e)), although the nanoparticles are more subdiffusive than the polymers at low κ but less subdiffusive at high κ.[50] The long-time dynamics also strongly depend on κ. D/D_0 generally decreases with increasing σ_{NP}/ξ, consistent with CPR coupling, but the onset of the decrease in D/D_0 occurs at lower σ_{NP}/ξ as κ is increased (Figure 6(f)). This result suggests that structural heterogeneities in ring solutions play a significant role in the nanoparticle dynamics as the rings stiffen. Indeed, our simulations reveal pronounced structural changes upon increasing κ, with $R_{g,0}$ increasing monotonically and the shape transitioning from oblate-like to prolate-like; at sufficiently high κ, the nanoparticles can even occupy holes in the center of aligned, expanded rings (Figure 6(d) right). Nevertheless, the short-time dynamics of the nanoparticles and polymer centers-of-mass remain coupled across the range of stiffnesses examined.

In linear polymer solutions, increasing stiffness drives decoupling of the dynamics (Figure 6(g)) on both short and long time scales.[51] The subdiffusive exponents α_{NP} and α_P are linearly proportional at low polymer concentration (high α_P) but decouple at high polymer concentration, and the decrease in α_{NP} is more rapid as κ is increased (Figure 6(h)). Likewise, D/D_0 is consistent with the $(\sigma_{NP}/\xi)^{-2}$ scaling at low κ but decreases more rapidly as κ is increased (Figure 6(i)). These changes in diffusivity are reasonably captured by a variant of mode-coupling theory developed for dense polymer solutions,[36] and reflect slowing of the monomer dynamics for stiffer chains. Broadly, these results indicate that changes to the nature of polymer segmental relaxations significantly perturb the dynamic coupling controlling nanoparticle dynamics and transport.

NANOPARTICLE DYNAMICS IN CHARGED POLYMERS

To understand how chain conformation alters nanoparticle transport, we measured the dynamics of nanoparticles in solutions of a model strong polyelectrolyte, sodium poly(styrenesulfonate) (NaPSS).[52] The conformation of charged polymers differs from that of neutral polymers due to the electrostatic repulsions between charges along the polymer backbone, which lead to extended conformations.[53] In NaPSS solutions at high ionic strength ([NaCl] = 10^{-1} M), the diffusivities of polystyrene nanoparticles approximately follow the SES prediction across the dilute to semidilute regimes across a range of particle sizes (Figure 7(a)). Similarly, D/D_{SES} is approximately independent of c/c^* for large particles (diameter $\geq$300 nm) diffusing in NaPSS solutions without added salt (Figure 7(b)), again indicating that particles diffuse according to the solution viscosity. By contrast, D/D_{SES} depends non-monotonically on c/c^* for smaller (100 and 200 nm diameter) particles: it first increases up to $c/c^* \approx 10$ and subsequently decreases to approach 1 at higher concentrations. Because the polymer R_g is comparable to the particle size across this concentration range, we proposed that the particles are locally constrained by the heterogeneous polyelectrolyte structure in a fashion analogous to the constraints provided by entanglements,[8] leading to a return to SES diffusion at high concentrations. Notably, our results contrast with the concentration dependences observed for nanoparticles much smaller than ξ,[23] highlighting the importance of the relative size R_{NP}/ξ on the physical mechanisms controlling diffusion processes.

UNDERSTANDING SOFT INTERACTIONS VIA GRAFTED POLYMER DYNAMICS

To this point, the particles used in our studies were "hard" because the interaction potential contained a sharp excluded volume repulsion at the particle diameter. Particles with comparatively "soft" interactions have exciting applications in sensing, drug delivery, and functional coatings but their transport properties are corresponding less fundamentally understood. A common route to generating soft interparticle interactions is to graft polymers to the particle surface so that the steric, excluded volume, and electrostatic interactions of the grafted layer determine the steepness and range of the interparticle potential. The diffusion of polymer-grafted nanoparticles through polymer solutions and melts thus depends on the interactions between grafted polymers and free chains. For example, we showed that D/D_0 for grafted silica nanoparticles in PS solutions collapses onto a master curve using a modified version of CPR coupling $(R_h/\xi)(M_{w,f}/M_{w,g})^{3/8}$, where $M_{w,f}$ and $M_{w,g}$ are the molecular weights of the free and grafted chains, respectively (Figure 8).[54] Although we still do not understand the origin of the 3/8 factor, the ratio $M_{w,f}/M_{w,g}$ controls the nanoscale interactions that in turn dictate nanoparticle diffusion.

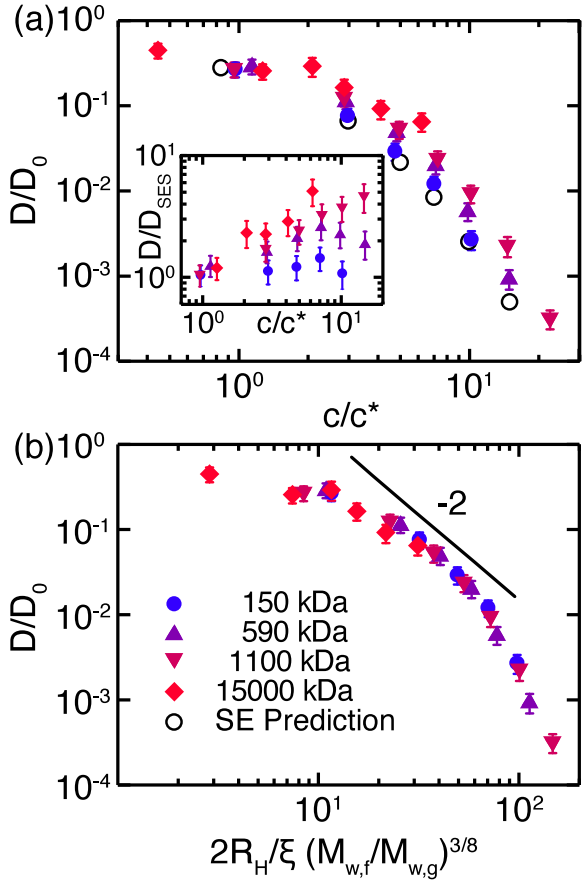


Figure 8. Normalized diffusivity D/D_0 as a function of (a) normalized free polymer concentration c/c^* and (b) scaling variable $(R_h/\xi)(M_{w,f}/M_{w,g})^{3/8}$ for polystyrene-grafted silica nanoparticles diffusing in solutions of polystyrene in 2-butanone. Open and closed colored symbols correspond to $M_{w,g}$ = 33 and 355 kDa, respectively. Inset to (a): D/D_{SES} versus c/c^*. Reproduced from ref 54. Copyright 2019 American Chemical Society.

https://doi.org/10.1021/accountsmr.6c00189
Acc. Mater. Res. XXXX, XXX, XXX−XXX

Downloaded from pubs.acs.org/amrcda/article-pdf/doi/10.1021/accountsmr.6c00189/6900609/accountsmr.6c00189.pdf by UNIV OF RHODE ISLAND user on 29 October 2026

To understand one mechanism thought to generate these altered dynamics, we conducted experiments and simulations to probe the relaxations of the grafted polymer chains themselves. Their dynamics differ from those in bulk polymer solutions because the chains experience intra- and interchain interactions and the tether restricts the conformational states accessible to the polymer. Indeed, neutron spin−echo spectroscopy measurements of PS chains (M_w = 355 kDa) grafted to silica nanoparticles revealed that the polymer dynamics do not exhibit the Zimm relaxations expected at these time and length scales (Figure 9(a)); instead, the grafted polymers relax more slowly

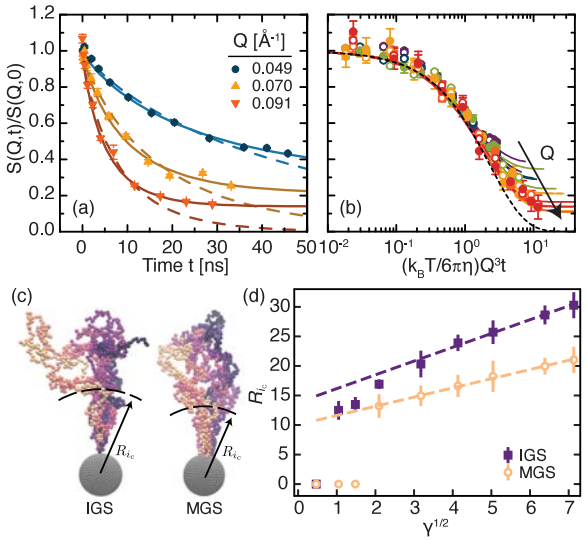


Figure 9. Polymer brushes exhibit confined dynamics that reflects a structural transition from the concentrated to semidilute polymer brush regimes. (a, b) Representative normalized dynamic correlation functions $S(Q, t)/S(Q, 0)$ (a) as a function of time t and (b) Zimm scaling plots for silica nanoparticles with grafted polystyrene chains (M_w = 355 kDa) over a wavevector range of 0.042 Å^{-1} ≤ Q ≤ 0.107 Å^{-1}. Dashed curves are best fits to an initial Zimm decay at short times. Solid curves are best fits to $S(Q, t) = (1 - f)\exp[-(\Gamma t)^{0.85}] + f$. Reproduced from ref 45. Copyright 2017 American Chemical Society. (c) Representative chain conformations for a single chain over n = 10 time points for IGS and MGS chains at γ = 50. (d) Scaling of the critical radius R_{i_c} at which monomers no longer exhibit a confinement plateau as a function of the square root of grafting density $\gamma^{1/2}$ for chains with IGS and MGS. (c) and (d) are reproduced from ref 55. Copyright 2026 American Chemical Society.

on long time scales and, surprisingly, exhibit long-time plateaus consistent with dynamics confined by neighboring chains and controlled by grafting density.[45] The height of the plateau, a measure of the extent of confinement, decreases with increasing wavevector, indicating that the polymers relax more slowly on longer length scales. Further, the confinement length calculated from the plateau height is in good agreement with the distance between grafted chains. Thus, confinement by neighboring chains restricts the dynamics of grafted polymers.

Neutron scattering methods are able to capture dynamics across a range of wavevectors and hence length scales, but cannot simply access the dynamics of individual monomers along the chain without careful synthesis and contrast-matching to generate scattering only from selected monomers.[56] Thus, we complemented the experiments with molecular simulations of brushes grafted to nanoparticles using our hybrid MD-MPCD approach (including long-range HI) and LD simulations (without long-range HI).[57] First, we generated immobile grafting sites (IGS), expected for brushes grafted to solid nanoparticles, and calculated the mean-square angular displacement (MSAD) $\langle[\theta_i(t)]^2\rangle$ of the ith monomer. Monomers near the particle surface exhibit plateaus in the MSADs on intermediate time scales, consistent with the NSE results[45] and indicative of confined dynamics. Beyond a critical monomer index i_c, the MSADs no longer exhibit plateaus and the monomers are thus effectively not confined by their neighbors. The average distance R_{i_c} of the critical monomer from the nanoparticle center depends on the grafting density according to $R_{i_c} \sim \gamma^{1/2}$. Astonishingly, the scaling of this dynamic length scale exactly follows the scaling predicted for the critical radius R_{CPB} that controls the transition between the concentrated and semidilute brush regimes using the extended Daoud-Cotton theory.[58,59] Thus, our models show that the dynamic confinement measured in simulations and experiments arises from a structural transition that, in turn, is due to weakening of the steric interactions that control chain extension.

Finally, we very recently relaxed the requirement that the grafting sites be immobile;[55] such mobile grafting sites (MGS) are found for polymers on the surfaces of emulsion drops, vesicles, and lipid bilayers. Brushes with MGS exhibit the same $R_{i_c} \sim \gamma^{1/2}$ scaling as for brushes with IGS but with smaller values of R_{i_c} (Figure 9(d)), indicating that tether mobility reduces dynamical confinement. To distinguish effects of crowding from those of mobility, we simulated brushes in which a fraction f of the grafting sites were MGS and the rest were IGS. R_{i_c} for the brushes with IGS decreases monotonically with f even though the brush structure is unaffected by the fraction of mobile chains, indicating that MGS chains dynamically facilitate relaxations of chains with fixed grafting sites. We expect that these confined relaxations of the grafted polymer play a significant role in how the polymer-grafted nanoparticles couple to segmental fluctuations in polymer solutions. For example, the confined dynamics of the grafted chains may result in a time-dependent length scale controlling the dynamic coupling, where the grafted polymer acts almost as a hard sphere on short time scales but softens to interpenetrate the fluctuating polymer mesh on longer length scales. The disparity in length and time scales between polymer fluctuations, confined relaxations, and particle translation, however, poses a significant barrier to establishing the direct theoretical relationship that connects these dynamics on different scales.

SUMMARY AND OUTLOOK

By combining microscopy and scattering experiments with simulations, we have identified factors that determine the dynamics of nanoparticles in solutions of comparably sized polymers. The long-time dynamics are controlled by relaxations of polymer segments of similar size, following predictions from scaling theory[8,33] and, at higher polymer concentrations, MCT.[36] On short time scales, we identified a coupling mode between the subdiffusion of the nanoparticles and the polymer centers-of-mass that arises because both objects relax on similar length and time scales. Our simulations further identified how chain conformation and stiffness affect these coupling mechanisms. As a step toward understanding the effects of soft interactions produced by grafted chains on transport, we showed that the transition from confined to unconfined dynamics along polymer brushes coincides with the structural

Downloaded from pubs.acs.org/amrcda/article-pdf/doi/10.1021/accountsmr.6c00189/6900609/accountsmr.6c00189.pdf by UNIV OF RHODE ISLAND user on 29 October 2026

https://doi.org/10.1021/accountsmr.6c00189
Acc. Mater. Res. XXXX, XXX, XXX−XXX

transition from concentrated to semidilute brush regimes. Both transitions are affected by the mobility of the grafting site, suggesting that chain mobility may affect the transport properties of emulsions, lipid bilayers, or vesicles functionalized with brushes. Together, our results rationalize the size dependence of nanoparticle transport in polymer solutions as models for heterogeneous soft materials and provide a framework by which to systematically elucidate the underlying mechanisms.

Remaining open questions that are likely to significantly advance the design of functional materials include:

- The role of *polymer topology* on the mechanisms of nanoparticle transport; for example, how nanoparticles diffuse in solutions of stars, dendrimers, bottlebrushes, and brush polymers as well as in hydrogels and networks[60−62] that are increasingly used in practical applications. We expect that fundamental understanding in these environments will require characterizing the distinct mechanisms by which hierarchically structured polymers relax on different length scales — for example, arm retraction in stars, side chain relaxation in bottlebrushes, or the relaxation of the strands between physical or chemical junctions in networks — and linking these relaxations to the dynamics measured for nanoparticles. This linkage is nontrivial, as shown by the example of grafted polymer dynamics and grafted nanoparticle dynamics, and likely requires advances in theory in parallel with carefully designed experiments and simulations to probe dynamics across scales.
- The role of *polymer charge* on coupling mechanisms, subdiffusion, and diffusive transport. Our studies revealed distinct mechanisms for nanoparticle transport in stiff versus charged polymers, related to the local persistence length and to structural heterogeneities in solutions of charged polymers. Identifying the mechanisms by which these physics differently affect transport processes has significant implications for the design of theranostics in drug delivery, for the processing of polymer nanocomposites, and the manufacturing of advanced coatings.
- The role of *nanoparticle shape* on coupling to polymer segmental versus center-of-mass dynamics. Nonspherical particles percolate at lower particle volume fractions than spheres, enabling functional properties that depend on connectivity (for example, electrical or thermal transport), motivating studies of their transport properties. Anisotropic particles couple differently to polymer relaxations along and normal to their long axis.[63,64] Whereas the rotational diffusion of short nanorods couples directly to solution viscoelasticity,[65] we have recently found that the diffusion of flexible, anisotropic bacteriophage couples to the dynamics of DNA molecules and not to the bulk viscoelasticity.[66] The central question is to understand when anisotropic probes couple to segmental relaxations versus center of mass motion versus bulk viscoelasticity.
- The role of *time-dependent polymer dynamics* on the dynamics of nanoparticles. For example, transient associations or stickers enable the reprocessing or recycling of polymer-based materials and composites. Similarly, time-dependent bulk rheological properties such as thixotropy (the recovery of elasticity as the complex fluid restructures after stress is applied) enable self-healing. We expect that diffusive transport and hence the spatial distribution of nanoparticles will change over time as the microscopic associations and/or structure of the polymers evolve. How to connect the changes in dynamics to the evolution of polymer properties remains understudied, especially in well-controlled models that may provide fundamental insight into mechanisms.
- The dynamics *out of equilibrium*. This Account focuses on materials near thermodynamic equilibrium, in which transport is driven by thermal or concentration fluctuations. Processing polymer solutions and solids under nonequilibrium conditions, as required for applications in printing, spraying, and coating, among others, changes the material structure and relaxation spectra. How nanoparticle dynamics couple to these perturbations from equilibrium is essential to develop and preserve function during processing.

AUTHOR INFORMATION

Corresponding Authors

Jacinta C. Conrad − *Department of Chemical and Biomolecular Engineering, University of Houston, Houston, Texas 77204, United States;* orcid.org/0000-0001-6084-4772; Email: jcconrad@uh.edu

Ryan Poling-Skutvik − *Department of Chemical, Biomolecular, and Materials Engineering and Department of Physics, University of Rhode Island, Kingston, Rhode Island 02881, United States;* orcid.org/0000-0002-1614-1647; Email: ryanps@uri.edu

Jeremy C. Palmer − *Department of Chemical and Biomolecular Engineering, University of Houston, Houston, Texas 77204, United States;* orcid.org/0000-0003-0856-4743; Email: jcpalmer@uh.edu

Authors

Mohammadjavad Haji Rezaei − *Department of Chemical, Biomolecular, and Materials Engineering, University of Rhode Island, Kingston, Rhode Island 02881, United States;* orcid.org/0009-0001-4383-8984

Shivraj B. Kotkar − *Department of Chemical and Biomolecular Engineering, University of Houston, Houston, Texas 77204, United States;* orcid.org/0000-0001-6051-9363

Complete contact information is available at: https://pubs.acs.org/10.1021/accountsmr.6c00189

Notes

The authors declare no competing financial interest.

Biographies

Jacinta C. Conrad is Professor of Chemical and Biomolecular Engineering at the University of Houston (UH). She holds an SB in Mathematics from the University of Chicago and MA and PhD degrees in Physics from Harvard. Her research focuses on transport in complex fluids and soft materials.

Ryan Poling-Skutvik is Associate Professor of Chemical, Biomolecular, and Materials Engineering at the University of Rhode Island (URI). He received a B.E. from The Cooper Union for the Advancement of Science and Art and a Ph.D. from UH, both in Chemical Engineering. His research group focuses on developing relationships between structure, dynamics, and properties in soft materials.

Downloaded from pubs.acs.org/amrcda/article-pdf/doi/10.1021/accountsmr.6c00189/6900460/accountsmr.6c00189.pdf by UNIV OF RHODE ISLAND user on 29 October 2026

Mohammadjavad Haji Rezaei is a PhD candidate in Chemical, Biomolecular, and Materials Engineering at URI. He received B.S. and M.S. degrees in Materials Science and Engineering from Sharif University of Technology. His research focuses on polymer physics and soft matter.

Shivraj B. Kotkar is a postdoctoral fellow in Chemical and Biomolecular Engineering at UH, where he earned a Ph.D. in Chemical Engineering. He received B.Tech and M.Tech. degrees in Chemical Engineering from IIT Kharagpur. His research focuses on understanding dynamics of soft matter systems using molecular simulations.

Jeremy C. Palmer is Professor of Chemical and Biomolecular Engineering at UH. He earned a BS in Biomedical Engineering from Johns Hopkins University and a PhD in Chemical Engineering from North Carolina State University. His research focuses on modeling and simulation of complex fluids and soft materials.

■ ACKNOWLEDGMENTS

This work was supported by the Welch Foundation [E-1869 (J. C. C.) and 1882 (J. C. P.)], the National Science Foundation [CBET-2437846 (J. C. C.) and CBET-2529134 (J. C. C. and J. C. P.)], and a Cottrell Scholar Award #CS-CSA-2025-033 from Research Corporation for Science Advancement (R. P.-S.). Computational resources for the studies described herein were provided by the Hewlett-Packard Enterprise Data Science Institute at the University of Houston and the Texas Advanced Computing Center at the University of Texas at Austin. We also thank numerous collaborators and colleagues for helpful discussions over the years, especially Michael Howard, Ramanan Krishnamoorti, Amanda Marciel, and Arash Nikoubashman.

■ REFERENCES

(1) Wong, C.; Stylianopoulos, T.; Cui, J.; Martin, J.; Chauhan, V. P.; Jiang, W.; Popović, Z.; Jain, R. K.; Bawendi, M. G.; Fukumura, D. Multistage Nanoparticle Delivery System for Deep Penetration into Tumor Tissue. *Proc. Natl. Acad. Sci. U.S.A.* **2011**, *108*, 2426−2431.

(2) Ensign, L. M.; Henning, A.; Schneider, C. S.; Maisel, K.; Wang, Y.-Y.; Porosoff, M. D.; Cone, R.; Hanes, J. *Ex Vivo* Characterization of Particle Transport in Mucus Secretions Coating Freshly Excised Mucosal Tissues. *Mol. Pharmaceutics* **2013**, *10*, 2176−2182.

(3) Johansson, J. M.; Du Rietz, H.; Hedlund, H.; Eriksson, H. C.; Oude Blenke, E.; Pote, A.; Harun, S.; Nordenfelt, P.; Lindfors, L.; Wittrup, A. Cellular and Biophysical Barriers to Lipid Nanoparticle Mediated Delivery of RNA to the Cytosol. *Nat. Commun.* **2025**, *16*, 5354.

(4) Han, D.-Y.; Kim, S.; Kim, Y.; Lim, H.; Lee, G. R.; Song, C. K.; Song, W.-J.; Moon, H. C.; Park, S.; Park, T. Regulating Segmental Dynamics for Ion Clusters in Polymer Binders to Realize High-Areal-Capacity Electrodes in Lithium Batteries. *Energy Environ. Sci.* **2025**, *18*, 7514−7526.

(5) Bhattacharya, S.; Sharma, D. K.; Saurabh, S.; De, S.; Sain, A.; Nandi, A.; Chowdhury, A. Plasticization of Poly(Vinylpyrrolidone) Thin Films under Ambient Humidity: Insight from Single-Molecule Tracer Diffusion Dynamics. *J. Phys. Chem. B* **2013**, *117*, 7771−7782.

(6) Chakraborty, A.; Sutar, P.; Yadav, P.; Eswaramoorthy, M.; Maji, T. K. Charge-Assisted Self-Assembly of ZIF-8 and Laponite Clay toward a Functional Hydrogel Nanocomposite. *Inorg. Chem.* **2018**, *57*, 14480−14483.

(7) Sato, Y. K.; Kuwauchi, Y.; Miyoshi, W.; Jinnai, H. Visualization of Chemical Bonding in a Silica-Filled Rubber Nanocomposite Using STEM-EELS. *Sci. Rep* **2020**, *10*, 21558.

(8) Brochard Wyart, F.; de Gennes, P. G. Viscosity at small scales in polymer melts. *Eur. Phys. J. E* **2000**, *1*, 93−97.

(9) Rubinstein, M.; Colby, R. H. *Polymer Physics*; Oxford University Press: Oxford, NY, 2003.

(10) Teraoka, I. *Polymer Solutions*; John Wiley & Sons, Ltd, 2002.

(11) Mason, T. G.; Weitz, D. A. Optical Measurements of Frequency-Dependent Linear Viscoelastic Moduli of Complex Fluids. *Phys. Rev. Lett.* **1995**, *74*, 1250−1253.

(12) Squires, T. M.; Mason, T. G. Fluid Mechanics of Microrheology. *Annu. Rev. Fluid Mech.* **2010**, *42*, 413−438.

(13) Chapman, C. D.; Lee, K.; Henze, D.; Smith, D. E.; Robertson-Anderson, R. M. Onset of Non-Continuum Effects in Microrheology of Entangled Polymer Solutions. *Macromolecules* **2014**, *47*, 1181−1186.

(14) Yamamoto, U.; Schweizer, K. S. Microscopic theory of the long-time diffusivity and intermediate-time anomalous transport of a nanoparticle in polymer melts. *Macromolecules* **2015**, *48*, 152−163.

(15) Ye, X.; Tong, P.; Fetters, L. J. Transport of probe particles in semidilute polymer solutions. *Macromolecules* **1998**, *31*, 5785−5793.

(16) Cheng, Y.; Prud'homme, R. K.; Thomas, J. L. Diffusion of Mesoscopic Probes in Aqueous Polymer Solutions Measured by Fluorescence Recovery after Photobleaching. *Macromolecules* **2002**, *35*, 8111−8121.

(17) Tuteja, A.; Mackay, M. E.; Narayanan, S.; Asokan, S.; Wong, M. S. Breakdown of the continuum Stokes-Einstein relation for nanoparticle diffusion. *Nano Lett.* **2007**, *7*, 1276−1281.

(18) Holyst, R.; Bielejewska, A.; Szymański, J.; Wilk, A.; Patkowski, A.; Gapiński, J.; Zywociński, A.; Kalwarczyk, T.; Kalwarczyk, E.; Tabaka, M.; Ziebacz, N.; Wieczorek, S. A. Scaling form of viscosity at all length-scales in poly(ethylene glycol) solutions studied by fluorescence correlation spectroscopy and capillary electrophoresis. *Phys. Chem. Chem. Phys.* **2009**, *11*, 9025−9032.

(19) Kalwarczyk, T.; Ziębacz, N.; Bielejewska, A.; Zaboklicka, E.; Koynov, K.; Szymański, J.; Wilk, A.; Patkowski, A.; Gapiński, J.; Butt, H.-J.; Hołyst, R. Comparative Analysis of Viscosity of Complex Liquids and Cytoplasm of Mammalian Cells at the Nanoscale. *Nano Lett.* **2011**, *11*, 2157−2163.

(20) Kohli, I.; Mukhopadhyay, A. Diffusion of nanoparticles in semidilute polymer solutions: effect of different length scales. *Macromolecules* **2012**, *45*, 6143−6149.

(21) Nath, P.; Mangal, R.; Kohle, F.; Choudhury, S.; Narayanan, S.; Wiesner, U.; Archer, L. A. Dynamics of Nanoparticles in Entangled Polymer Solutions. *Langmuir* **2018**, *34*, 241−249.

(22) Bailey, E. J.; Griffin, P. J.; Composto, R. J.; Winey, K. I. Multiscale Dynamics of Small, Attractive Nanoparticles and Entangled Polymers in Polymer Nanocomposites. *Macromolecules* **2019**, *52*, 2181−2188.

(23) Senanayake, K. K.; Shokeen, N.; Fakhrabadi, E. A.; Liberatore, M. W.; Mukhopadhyay, A. Diffusion of nanoparticles within a semidilute polyelectrolyte solution. *Soft Matter* **2019**, *15*, 7616−7622.

(24) Hess, M.; Gratz, M.; Remmer, H.; Webers, S.; Landers, J.; Borin, D.; Ludwig, F.; Wende, H.; Odenbach, S.; Tschöpe, A.; Schmidt, A. M. Scale-dependent particle diffusivity and apparent viscosity in polymer solutions as probed by dynamic magnetic nanorheology. *Soft Matter* **2020**, *16*, 7562−7575.

(25) Jouault, N.; Moll, J. F.; Meng, D.; Windsor, K.; Ramcharan, S.; Kearney, C.; Kumar, S. K. Bound Polymer Layer in Nanocomposites. *ACS Macro Lett.* **2013**, *2*, 371−374.

(26) Griffin, P. J.; Bocharova, V.; Middleton, L. R.; Composto, R. J.; Clarke, N.; Schweizer, K. S.; Winey, K. I. Influence of the Bound Polymer Layer on Nanoparticle Diffusion in Polymer Melts. *ACS Macro Lett.* **2016**, *5*, 1141−1145.

(27) Won, J.; Onyenemezu, C.; Miller, W. G.; Lodge, T. P. Diffusion of Spheres in Entangled Polymer Solutions: A Return to Stokes-Einstein Behavior. *Macromolecules* **1994**, *27*, 7389−7396.

(28) Ogston, A. G.; Preston, B. N.; Wells, J. D. On the transport of compact particles through solutions of chain-polymers. *Proc. R. Soc. London A* **1973**, *333*, 297−316.

(29) Altenberger, A. R.; Tirrell, M.; Dahler, J. S. Hydrodynamic screening and particle dynamics in porous media, semidilute polymer solutions and polymer gels. *J. Chem. Phys.* **1986**, *84*, 5122−5130.

(30) Cukier, R. I. Diffusion of Brownian spheres in semidilute polymer solutions. *Macromolecules* **1984**, *17*, 252−255.

(31) Phillies, G. D. J.; Ullmann, G. S.; Ullmann, K.; Lin, T.-H. Phenomenological scaling laws for semidilute macromolecule solutions

Downloaded from pubs.acs.org/amrcda/article-pdf/doi/10.1021/accountsmr.6c00189/6900460/accountsmr.6c00189.pdf by UNIV OF RHODE ISLAND user on 29 October 2026

https://doi.org/10.1021/accountsmr.6c00189
Acc. Mater. Res. XXXX, XXX, XXX−XXX

from light scattering by optical probe particles. *J. Chem. Phys.* **1985**, *82*, 5242.
(32) Ziębacz, N.; Wieczorek, S. A.; Kalwarczyk, T.; Fiałkowski, M.; Hołyst, R. Crossover regime for the diffusion of nanoparticles in polyethylene glycol solutions: influence of the depletion layer. *Soft Matter* **2011**, *7*, 7181−7186.
(33) Cai, L.-H.; Panyukov, S.; Rubinstein, M. Mobility of nonsticky nanoparticles in polymer liquids. *Macromolecules* **2011**, *44*, 7853−7863.
(34) Ge, T. Scaling Perspective on Dynamics of Nanoparticles in Polymers: Length- and Time-Scale Dependent Nanoparticle−Polymer Coupling. *Macromolecules* **2023**, *56*, 3809−3837.
(35) Miyazaki, K.; Bagchi, B.; Yethiraj, A. Self-consistent mode-coupling theory for the viscosity of rodlike polyelectrolyte solutions. *J. Chem. Phys.* **2004**, *121*, 8120−8127.
(36) Egorov, S. A. Anomalous nanoparticle diffusion in polymer solutions and melts: A mode-coupling theory study. *J. Chem. Phys.* **2011**, *134*, 84903.
(37) Yamamoto, U.; Schweizer, K. S. Theory of nanoparticle diffusion in unentangled and entangled polymer melts. *J. Chem. Phys.* **2011**, *135*, 224902.
(38) Babaye Khorasani, F.; Poling-Skutvik, R.; Krishnamoorti, R.; Conrad, J. C. Mobility of Nanoparticles in Semidilute Polyelectrolyte Solutions. *Macromolecules* **2014**, *47*, 5328−5333.
(39) Poling-Skutvik, R.; Krishnamoorti, R.; Conrad, J. C. Size-Dependent Dynamics of Nanoparticles in Unentangled Polyelectrolyte Solutions. *ACS Macro Lett.* **2015**, *4*, 1169−1173.
(40) Mackay, M. E.; Dao, T. T.; Tuteja, A.; Ho, D. L.; van Horn, B.; Kim, H.-C.; Hawker, C. J. Nanoscale effects leading to non-Einstein-like decrease in viscosity. *Nat. Mater.* **2003**, *2*, 762−766.
(41) Sprakel, J.; van der Gucht, J.; Cohen Stuart, M. A.; Besseling, N. A. M. Rouse dynamics of colloids bound to polymer networks. *Phys. Rev. Lett.* **2007**, *99*, 208301.
(42) Poling-Skutvik, R.; Mongcopa, K. I. S.; Faraone, A.; Narayanan, S.; Conrad, J. C.; Krishnamoorti, R. Structure and Dynamics of Interacting Nanoparticles in Semidilute Polymer Solutions. *Macromolecules* **2016**, *49*, 6568−6577.
(43) Guo, H.; Bourret, G.; Lennox, R. B.; Sutton, M.; Harden, J. L.; Leheny, R. L. Entanglement-controlled subdiffusion of nanoparticles within concentrated polymer solutions. *Phys. Rev. Lett.* **2012**, *109*, 055901.
(44) Chen, R.; Poling-Skutvik, R.; Nikoubashman, A.; Howard, M. P.; Conrad, J. C.; Palmer, J. C. Coupling of nanoparticle dynamics to polymer center-of-mass motion in semidilute polymer solutions. *Macromolecules* **2018**, *51*, 1865−1872.
(45) Poling-Skutvik, R.; Olafson, K. N.; Narayanan, S.; Stingaciu, L.; Faraone, A.; Conrad, J. C.; Krishnamoorti, R. Confined Dynamics of Grafted Polymer Chains in Solutions of Linear Polymer. *Macromolecules* **2017**, *50*, 7372−7379.
(46) Howard, M. P.; Nikoubashman, A.; Palmer, J. C. Modeling hydrodynamic interactions in soft materials with multiparticle collision dynamics. *Current Opinion in Chemical Engineering* **2019**, *23*, 34−43.
(47) Malevanets, A.; Kapral, R. Mesoscopic Model for Solvent Dynamics. *J. Chem. Phys.* **1999**, *110*, 8605−8613.
(48) Chen, R.; Kotkar, S. B.; Poling-Skutvik, R.; Howard, M. P.; Nikoubashman, A.; Conrad, J. C.; Palmer, J. C. Nanoparticle dynamics in semidilute polymer solutions: Rings versus linear chains. *J. Rheol.* **2021**, *65*, 745−755.
(49) Sorichetti, V.; Hugouvieux, V.; Kob, W. Determining the Mesh Size of Polymer Solutions via the Pore Size Distribution. *Macromolecules* **2020**, *53*, 2568−2581.
(50) Kotkar, S. B.; Poling-Skutvik, R.; Howard, M. P.; Nikoubashman, A.; Conrad, J. C.; Palmer, J. C. Dynamics of Nanoparticles in Solutions of Semiflexible Ring Polymers. *J. Phys. Chem. B* **2024**, *128*, 12586−12596.
(51) Chen, R.; Poling-Skutvik, R.; Howard, M. P.; Nikoubashman, A.; Egorov, S. A.; Conrad, J. C.; Palmer, J. C. Influence of polymer flexibility on nanoparticle dynamics in semidilute solutions. *Soft Matter* **2019**, *15*, 1260−1268.
(52) Slim, A. H.; Poling-Skutvik, R.; Conrad, J. C. Local Confinement Controls Diffusive Nanoparticle Dynamics in Semidilute Polyelectrolyte Solutions. *Langmuir* **2020**, *36*, 9153−9159.
(53) Degiorgio, V.; Mantegazza, F.; Piazza, R. Transient Electric Birefringence Measurement of the Persistence Length of Sodium Polystyrene Sulfonate. *Europhys. Lett.* **1991**, *15*, 75−80.
(54) Poling-Skutvik, R.; Slim, A. H.; Narayanan, S.; Conrad, J. C.; Krishnamoorti, R. Soft Interactions Modify the Diffusive Dynamics of Polymer-Grafted Nanoparticles in Solutions of Free Polymer. *ACS Macro Lett.* **2019**, *8*, 917−922.
(55) Kotkar, S. B.; Howard, M. P.; Nikoubashman, A.; Conrad, J. C.; Palmer, J. C.; Poling-Skutvik, R. Mobile Grafts Allow Polymers to Escape Confinement. *ACS Macro Lett.* **2026**, *15*, 885−890.
(56) Wei, Y.; Xu, Y.; Faraone, A.; Hore, M. J. A. Local Structure and Relaxation Dynamics in the Brush of Polymer-Grafted Silica Nanoparticles. *ACS Macro Lett.* **2018**, *7*, 699−704.
(57) Kotkar, S. B.; Howard, M. P.; Nikoubashman, A.; Conrad, J. C.; Poling-Skutvik, R.; Palmer, J. C. Confined Dynamics in Spherical Polymer Brushes. *ACS Macro Lett.* **2023**, *12*, 1503−1509.
(58) Daoud, M.; Cotton, J. Star shaped polymers: a model for the conformation and its concentration dependence. *Journal de physique* **1982**, *43*, 531−538.
(59) Ohno, K.; Morinaga, T.; Takeno, S.; Tsujii, Y.; Fukuda, T. Suspensions of Silica Particles Grafted with Concentrated Polymer Brush: Effects of Graft Chain Length on Brush Layer Thickness and Colloidal Crystallization. *Macromolecules* **2007**, *40*, 9143−9150.
(60) Sorichetti, V.; Hugouvieux, V.; Kob, W. Dynamics of Nanoparticles in Polydisperse Polymer Networks: from Free Diffusion to Hopping. *Macromolecules* **2021**, *54*, 8575−8589.
(61) Moncure, P. J.; Millstone, J. E.; Laaser, J. E. Role of Ligand Shell Density in the Diffusive Behavior of Nanoparticles in Hydrogels. *J. Phys. Chem. B* **2023**, *127*, 9366−9377.
(62) Lv, Z.; Zhao, H.; Li, Z.; Qu, J.; Yang, S.; Liu, Y.; Zhang, W.; Zhang, L.; Yue, T.; Liu, J. Unveiling Nanoparticle Diffusion Mechanisms Confined in Different Polymer Topologies. *Macromolecules* **2025**, *58*, 11017−11028.
(63) Chen, Y.; Xiang, Z.; Ren, H.; Guo, F.; Ganesan, V.; Liu, J. Anisotropic and Non-Gaussian Diffusion of Thin Nanorods in Polymer Networks. *Macromolecules* **2024**, *57*, 5105−5118.
(64) Yari, S.; Haji Rezaei, M.; Chowning, L.; Roxbury, D.; Poling-Skutvik, R. Nanoscale anisotropy of SWCNTs promotes enhanced diffusion in heterogeneous complex fluids. *ACS Appl. Nano. Mater.* **2026**, *9*, 19812−19820.
(65) Molaei, M.; Atefi, E.; Crocker, J. C. Nanoscale Rheology and Anisotropic Diffusion Using Single Gold Nanorod Probes. *Phys. Rev. Lett.* **2018**, *120*, 118002.
(66) Safi Samghabadi, F.; Marfai, J.; Cueva, C.; Aporvari, M.; Neill, P.; Chabi, M.; Robertson-Anderson, R. M.; Conrad, J. C. Phage probes couple to DNA relaxation dynamics to reveal universal behavior across scales and regimes. *Soft Matter* **2025**, *21*, 935−947.

Downloaded from pubs.acs.org/amrcda/article-pdf/doi/10.1021/accountsmr.6c00189/6900609/accountsmr.6c00189.pdf by UNIV OF RHODE ISLAND user on 29 October 2026

https://doi.org/10.1021/accountsmr.6c00189
Acc. Mater. Res. XXXX, XXX, XXX−XXX